Genes, Brain and Behavior (2004) **3:** 273–286

Turning behavior in *Drosophila* larvae: a role for the small *scribbler* transcript

M. L. Suster[†,§], S. Karunanithi[‡,¶], H. L. Atwood[‡] and M. B. Sokolowski*,[†]

[†]*Department of Zoology, University of Toronto, Mississauga L5L 1C6,* [‡]*Department of Physiology, University of Toronto, Toronto ON, M5S 1A8,* [§]*McGill Centre for Research in Neuroscience, MGH Neurology L7-120, 1650 Cedar Avenue, Montreal, QC H3G 1A, Canada,* [¶]*Arizona Research Laboratories Division of Neurobiology, University of Arizona, Tucson, AZ 85721 USA*
**Corresponding Author: M. B. Sokolowski, Department of Biology, University of Toronto at Mississauga, Mississauga, Ontario, L5L 1C6,Canada. E-mail: msokolow@utm.utoronto.ca*

The *Drosophila* larva is extensively used for studies of neural development and function, yet the mechanisms underlying the appropriate development of its stereotypic motor behaviors remain largely unknown. We have previously shown that mutations in scribbler (*sbb*), a gene encoding two transcripts widely expressed in the nervous system, cause abnormally frequent episodes of turning in the third instar larva. Here we report that hypomorphic *sbb* mutant larvae display aberrant turning from the second instar stage onwards. We focus on the smaller of the two *sbb* transcripts and show that its panneural expression during early larval life, but not in later larval life, restores wild type turning behavior. To identify the classes of neurons in which this *sbb* transcript is involved, we carried out transgenic rescue experiments. Targeted expression of the small *sbb* transcript using the *cha*-GAL4 driver was sufficient to restore wild type turning behavior. In contrast, expression of this *sbb* transcript in motoneurons, sensory neurons or large numbers of unidentified interneurons was not sufficient. Our data suggest that the expression of the smaller *sbb* transcript may be needed in a subset of neurons for the maintenance of normal turning behavior in *Drosophila* larvae.

Keywords: *Drosophila*, genetics, development of turning behavior

Received 20 January 2004, revised 20 April 2004, accepted for publication 4 May 2004

Locomotion is generated by specialized networks of neurons, including premotor interneurons (located in the brain and spinal cord) and sensory neurons (located in the periphery), that drive patterned discharges in motoneurons to appropriate muscles (reviewed in Grillner 1985; Marder & Bucher 2001). While much is known about the physiological mechanisms by which neural networks generate locomotion, the genetic mechanisms underlying the assembly and maturation of locomotor networks are not well understood. Genes controlling the development of locomotor networks likely encode transcription factors and cell adhesion molecules that modify the synaptic connections and/or electrical properties of key neurons within the network (reviewed in Bate 1999; Marder 2000). An important challenge is to identify molecules regulating motor development in model organisms amenable to genetic manipulation. Behavioral screens in zebrafish have elegantly illustrated the use of genetic screens to uncover molecules required for the development of neural elements underlying swimming and escape behaviors (Granato *et al*. 1996; Ribera & Nusslein-Volhard 1998; reviewed in Fetcho & Liu 1998).

We are using the *Drosophila melanogaster* larva to identify genes involved in the development of neural elements underlying a stereotypic crawling behavior. *Drosophila* larvae crawl over substrates by alternating between rhythmic waves of peristalsis and brief episodes of head swinging and turning (Berrigan & Pepin 1995; Wang *et al*. 1997). A genetic screen for defects in third instar larval locomotion revealed scribbler (*sbb*), a gene required for wild type turning behavior (Shaver *et al*. 2000). Mutant larvae display abnormally frequent episodes of head swinging and turning in the third instar larval stage. *sbb* [also named brakeless (*bks*) in Senti *et al*. 2000] encodes two predominant transcripts (3.6 kb and 10.5 kb long) widely expressed in the nervous system and imaginal discs (Yang *et al*. 2000). Expression of the small *sbb* transcript in the nervous system alone was sufficient to rescue aberrant turning behavior in third instar *sbb* hypomorphic mutant larvae (Yang *et al*. 2000). *sbb* has been implicated in axon guidance (Rao *et al*. 2000; Senti *et al*. 2000) and cell proliferation/differentiation (Funakoshi *et al*. 2001; LaJeunesse *et al*. 2001). *sbb* transcripts encode novel nuclear proteins that contain several conserved domains found in vertebrate proteins. The large SBB protein contains a novel C2H2 type Zn^{+2} finger domain that is also encoded in frog, zebrafish, mouse and human transcripts; the smaller SBB protein does not contain this domain (Senti *et al*. 2000). Recent studies indicate that SBB likely acts as a transcriptional regulator (Funakoshi *et al*. 2001; Kaminker *et al*. 2002). How *sbb* contributes to the development of

doi: 10.1111/j.1601-183X.2004.00082.x

normal turning in third instar larvae is not known. Here we continue to use the small *sbb* transcript to begin an investigation into the developmental and neural origin of aberrant locomotion in *sbb* mutant larvae.

Materials and methods

Fly strains

Flies were raised in plastic vials containing standard fly medium (Ashburner 1989) and maintained at $24 \pm 1\,^{\circ}$C on a 12 h light/dark cycle and 50–80% humidity. Strains used were: *Canton-S* (*CS*; Würzburg, Germany); *white (w)*; *CS*, *Oregon-R* (*OR*; Cambridge, UK). Recessive lethal mutations were maintained in a *white* (*w*) background over green fluorescent protein (GFP)-labeled balancers, *CyO {actin-GFP}* (CyO^{GFP}) or *TM3, Ser {actin-GFP}* ($TM3,Ser^{GFP}$) to identify homozygous mutant animals (Bloomington Stock Center, Bloomington, IN). Most of the mutant alleles used in this study are larval or pupal-lethal mutations that have been previously described and some have been re-named (Fig. 2a) to simplify presentation. bks^1 (sbb^1) is a protein null allele (Senti *et al.* 2000). bks^4 is a small 436 bp deletion within the third exon (sbb^4 in Fig. 2a) and also a protein null allele (Rao *et al.* 2000). Pupal-lethal P{*lacZ*} enhancer-traps include *l(2)03432*; *rosy* (sbb^3; *ry*), *l(2)k04440* (sbb^5), *l(2)k00702* (sbb^6) (Yang *et al.* 2000). P-elements *w*; *EP(2)0328* (Yang *et al.* 2000) and *w*; *EP(2)2461* (inserted 538 bp upstream of the *sbb* ATG start site, obtained from Exelixis Inc, San Francisco, CA) are viable insertions in *sbb*. *Df(2R)Pc4* is a second chromosome deficiency with breakpoints at 55A and 55F, and *Df(2R)J2* is a >10 kb deletion generated by imprecise excision of *l(2)03432* (Yang *et al.* 2000). sbb^{256} and sbb^{324} are lethal nonsense point mutations (amino acid 1899 and 1608, respectively) in the 10.5 kb transcript (LaJeunesse *et al.* 2001). A transgene encoding the 3.6 kb *sbb* cDNA (*sbb3.6*) under the control of the heat shock promoter (*hs-sbb3.6*) was previously introduced into the sbb^3 mutant background (Yang *et al.* 2000).

Most strains used for targeted gene expression with the GAL4/Upstream activating sequence (UAS) system (Brand & Perrimon 1993; see *Results* for more details about the GAL4/UAS system) are described below. We examined the expression pattern of all GAL4 'drivers' used by crossing these to UAS 'responder' lines encoding one of the following reporter proteins: a fusion of mouse antigen CD8 and GFP (*UAS-mCD8-GFP*; Lee & Luo 1999), a fusion of TAU and β-*gal* (*UAS-tau-lacZ*; Lee & Luo 1999) and a nuclear GFP and β-*gal* fusion (*UAS-GFP-NlacZ*; Shiga *et al.* 1996). *UAS-mCD8-GFP* was introduced into the *Df(2R)J2* null background to generate *w*; $Df(2R)J2/CyO^{GFP.}$; *UAS-mCD8-GFP* (Fig. 4). Other UAS lines used include *w*; *UAS-tetanus toxin light chain* (TNT-G), which encodes a neural-specific toxin that blocks evoked synaptic vesicle release (Sweeney *et al.* 1995), and *w; UAS-electrical knockout* (*EKO*), which encodes a GFP-tagged non-inactivating Shaker K^+ channel (White *et al.* 2001). Flies carrying a fusion of the eye-specific enhancer, *glass* multimer reporter (GMR), and the cell death gene *head involution defective* (*hid*) were obtained from the Bloomington Stock Center (pGMR-*hid*).

Construction of fly strains for GAL4/UAS rescue

A third chromosome, homozygous viable UAS transgene encoding the 3.6 kb *sbb* cDNA (*UAS-sbb3.6*; Yang *et al.* 2000) was placed in the *w*; sbb^3 hypomorphic background. All GAL4 transgenes were placed in the sbb^3 mutant background by standard crosses using the *w*; lf/CyO^{GFP}; *MKRS/TM3*,Ser^{GFP} balancer stock, except for second chromosome-linked GAL4 transgenes that were recombined onto the sbb^3 chromosome. The expression patterns of GAL4 enhancer-traps or promoter-GAL4 lines (described below) were confirmed with several UAS reporter lines (see previous section) by antibody labeling and laser confocal microscopy. For GAL4 rescue experiments (Fig. 5a), flies carrying the *UAS-sbb3.6* transgene in the sbb^3 mutant background (*w*; sbb^3/CyO^{GFP}; *UAS-sbb3.6*) were crossed to flies carrying the GAL4 driver in the same mutant background. Each cross was replicated at least twice. Homozygous sbb^3 larvae could be distinguished from heterozygous sbb^3/CyO^{GFP} larvae by the absence of GFP fluorescence.

We used an enhancer-trap in the pan-neural *embryonic lethal abnormal vision* (*elav*) locus, *C155-GAL4* (Lin & Goodman 1994), to target *sbb* expression to all neurons. *cha-GAL4* is a 7.4 kb *choline acetyltransferase* promoter-GAL4 fusion and was used to drive expression in cholinergic neurons (Kitamoto 2001; Salvaterra & Kitamoto 2001). *Mz1060-GAL4* (kindly provided by K. Ito and J. Urban) and *l(3)-31-GAL4* (Brand & Perrimon 1993) were used to target *sbb* expression to all neuroblasts during embryonic and larval life (Fig. 5b). *teashirt* (*tsh*)-$GAL4^{MD741}$ (Calleja *et al.* 1996) drives expression in a large subset of ventral nerve cord interneurons, many neuroblasts and imaginal discs (Fig. 5b). *P0163-GAL4* was used to target expression to all embryonic and early larval sensory neurons (Suster & Bate 2002), and subsets of sensory neurons that persist into late larval stages (M. L. Suster, unpublished observations). *109(2)80-GAL4* labels a large proportion of sensory neurons, the multidendritic neurons and some chordotonal organs (Gao *et al.* 1999). *152.1-GAL4* labels the embryonic visual system (Münster Stock Center; M. L. Suster, unpublished observations). *fushi tarazu neurogenic* (ftz_{ng20})-*GAL4* labels all embryonic motoneurons (Thor *et al.* 1999), and both *D42-GAL4* (Gustafson & Boulianne 1996) and *OK6-GAL4* (Aberle *et al.* 2002) drive expression in larval motoneurons and subsets of interneurons (Fig. 5b and data not shown).

Dopamine decarboxylase (*Ddc*)-*GAL4* was used to target *sbb* expression to dopaminergic and serotonergic neurons (Li *et al.* 2000). To target *sbb* expression to peptidergic neurons we used *c929-GAL4*, which labels ~100 interneurons and neurosecretory cells, *386Y-GAL4* which labels a large number of interneurons (>200) and *36Y-GAL4* which labels a

small subset of central neurons including myomodulin interneurons (O'Brian & Taghert 1998; Taghert *et al*. 2001). *Feb296-GAL4*, *Kurz21-GAL4*, *Mai53-GAL4*, *Mai301-GAL4* label different sets of ring gland and peptidergic interneurons ($n > 100$ cells in each, Siegmund & Korge 2001). *reversed polarity* (*repo*)-*GAL4* labels virtually all glia (Sepp & Auld 1999) and *Mz840-GAL4* (Ito *et al*. 1995) labels a subset of glia (*interface glia* in Fig. 5a). The mesodermal driver *24B-GAL4* (Brand & Perrimon 1993), *Nervana1* (*Nrv1*)-*GAL4* (Sun *et al*. 2001) and *Myosin heavy chain* (*Mhc*)-*GAL4* (Zito *et al*. 1997) were used to target *sbb* expression to the embryonic and larval musculature. *hedgehog* (*hh*)-*GAL4* (Funakoshi *et al*. 2001) was used to target *sbb* expression to the epidermis, imaginal discs and developing visual system.

Construction of fly strains for GeneSwitch rescue

A transgene encoding a fusion of the pan-neural *elav* promoter and the coding sequence of the drug-inducible *GeneSwitch* activator (*elav-GeneSwitch*; Osterwalder *et al*. 2001) was placed in the sbb^3 mutant background. sbb^3/CyO^{GFP}; *elav-GeneSwitch* flies were crossed to sbb^3/CyO^{GFP}; *UAS-sbb3.6*. Embryos were collected from this cross and homozygous mutant sbb^3/sbb^3 larvae distinguished from heterozygous sbb^3/CyO^{GFP} controls by the absence of GFP fluorescence. Newly hatched larvae were collected within 1–2 h, aged from the time of hatching (h posthatch), and fed an RU486 analogue (mifeprestone, Sigma, Mississauga, ON, Canada) in yeast at a concentration of 50 μg/ml (Osterwalder *et al*. 2001).

Immunohistochemistry and confocal microscopy

Tissues were fixed for approx. 1 h in 4% paraformaldehyde in phosphate buffered saline (PBS), washed three times with PBS-TX (0.03% Triton-X 100 in 1X PBS) and incubated with a primary antibody overnight at 4 °C, diluted as follows: 1:100 for mouse antiβ-gal (Promega, Madison, WI), 1:50 for mouse anti-Brakeless (Fig. 3; Senti *et al*. 2000) or 1:200 for rabbit anti-Brakeless (Rao *et al*. 2000), 1:20 for rabbit anti-Tyrosine Hydroxylase (TH; Pel-Freez, Alabama), 1:100 for mouse 22C10 (see Suster & Bate 2002), 1:10 for mouse anti-Abnormal Chemosensory Jump 6 (ACJ6; see Certel *et al*. 2000), 1:500 for mouse anti-Choline Acetyl-Transferase (ChAT; Salvaterra and Kitamoto, 2001), 1:20 for mouse anti-Fasciclin II (FASII; see Zito *et al*. 1997), 1:100 for mouse anti-ELAV (Developmental Hybridoma Bank, IA, USA), 1:500 for rabbit anti-Reversed Polarity (REPO; see Senti *et al*. 2000), 1:1000 for rabbit anti-FMRFamide (Schneider *et al*. 1993), 1:30 for mouse anti-Even Skipped (EVE; see Certel *et al*. 2000), 1:750 for rabbit anti-Peptidylglycine-alpha-hydroxylating monooxygenase (PHM; see Taghert *et al*. 2001), 1:20 for rat antimouse CD8 (mCD8; CALTAG Laboratories, Burlingame, CA). After washing and blocking non-specific binding for 15 min, a secondary antibody, fluorescently conjugated (rabbit-FITC, Molecular probes; Cy2 and/or mouse Cy5, Jackson Laboratories, West Grove, PA) was added at 1:100 in PBS-TX with 5% horse serum for 45 min to 1 h. Tissues were immersed in 50% glycerol for 5 min and then mounted in 50% glycerol under a glass coverslip. Fluorescently labeled preparations were imaged using a Leica TCS SP (Fig. 3) or Zeiss LSM 510 (Figs 4 and 5) confocal microscope equipped with Kr/Ar/Ne lasers, except for those presented in Fig. 4d & d′ which were imaged using a Zeiss Axioscope and an attached Sony digital camera. Optical sections were obtained at 2–5 μm intervals, and when appropriate, reconstructed into 3D projections using Leica or Zeiss software. Final images were assembled in Adobe PHOTOSHOP.

Computer-assisted analysis of larval locomotion

Each larva was gently washed and allowed to crawl freely for 3 min on a 2.5% agar slab within a 13 cm diameter Petri dish (Suster *et al*. 2003). Crawling episodes were recorded at 22 ± 1 °C. Monochrome images of the crawling arena (768×768 pixels) were captured at ~1 frame/second using a monochrome digital camera on a 1GHz PC computer through the Northern Elite Image Analysis system (Empix Inc., Mississauga, ON, Canada). Movies were analyzed off-line using the Dynamic Image Analysis System (DIAS) that is commercially available from Solltech, Inc (Oakdale, IA). Speed (mm/second) and absolute turning rate (deg/second) were automatically obtained from DIAS (Wang *et al*. 1997). Linear locomotion episodes (straight moves) were defined as any episodes of at least 5 consecutive steps with an absolute turning rate ≤ 20 deg/second. Pause episodes were defined as any episodes in which turning rate was greater than 20 deg/second (Suster *et al*. 2003). Turning rate was calculated as direction change in deg/seconds and obtained directly from DIAS (Wang *et al*. 1997). Parameters were computed automatically with a program written in Visual BASIC (Suster *et al*. 2003) and compared using one-way analysis of variance (ANOVA) and the Student-Neuman-Keuls (SNK) a *posteriori* test in SPSS 6.0 (Macintosh; SPSS, Inc., Chicago, IL). The Student's *t*-test was used for statistical comparisons presented in Fig. 1 and in the text unless otherwise indicated. Data were plotted using EXCEL 2001 (Microsoft) and IGOR PRO 3.16 (Wavemetrics, Inc., Lake Oswego, OR).

Electrophysiology

Wandering third instar larvae were dissected in Schneider's insect medium (Sigma) along the dorsal midline and flattened (Jan & January 1976) using moveable magnetic retractors on a glass dish glued to magnetic film. The body-wall muscles and nervous system were exposed by removing the viscera; the segmental nerves were not cut. The preparation was continuously superfused with saline (HL3; Stewart *et al*. 1994) containing 1.5 mM Ca^{+2}, and the temperature was controlled by circulating the saline over a Peltier battery before it superfused the preparation. Excitatory junction potentials (EJPs) were recorded from muscle fiber 6, in abdominal segments 2 or 3, using 1.5 M KCl and 1.5 M

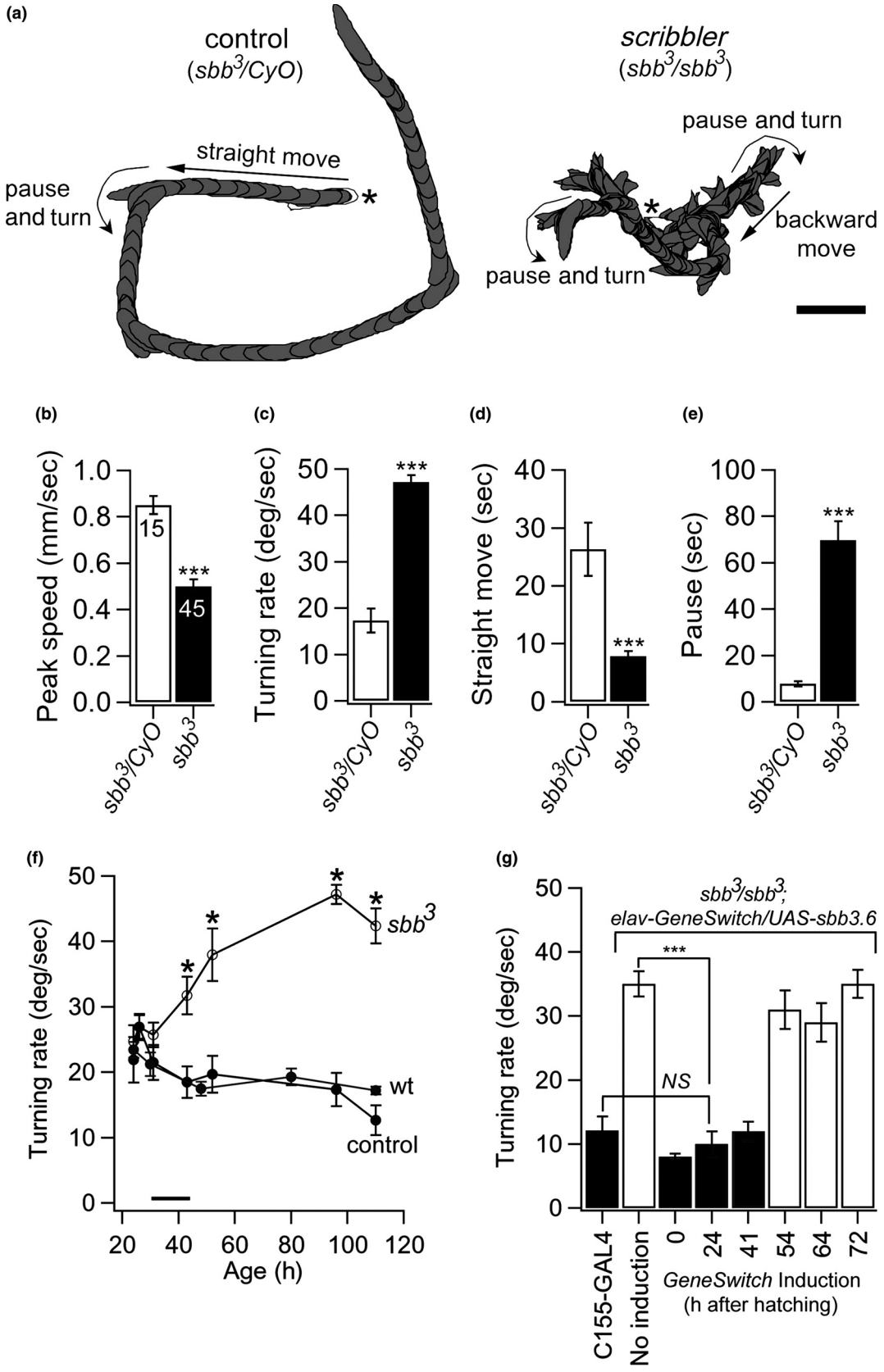
(a)
control
(sbb3/CyO)
straight move
pause
and turn
scribbler
(sbb3/sbb3)
pause and turn
backward
move
pause and turn
(b)
Peak speed (mm/sec)
15
45
***
sbb3/CyO
sbb3
(c)
Turning rate (deg/sec)
***
(d)
Straight move (sec)
***
(e)
Pause (sec)
***
(f)
Turning rate (deg/sec)
sbb3
wt
control
Age (h)
(g)
sbb3/sbb3;
elav-GeneSwitch/UAS-sbb3.6
***
NS
Turning rate (deg/sec)
C155-GAL4
No induction
0
24
41
54
64
72
GeneSwitch Induction
(h after hatching)

Figure 1: *scribbler* (*sbb*) mutant larvae show aberrant crawling patterns. Movies of crawling in heterozygous control (sbb^3/CyO^{GFP}) and *scribbler* (sbb^3/sbb^3) larvae (96 ± 4 h after hatching) were recorded for 3 min on a non-nutritive agar substrate. (a) Representative digital reconstructions of body outlines of control and *scribbler* mutant larvae generated and overlaid sequentially using DIAS (60 and 180 frames, respectively). The larval body outline in the first frame of the movie is shown unfilled (also labeled by an asterisk). Scale bar, 5 mm. Control larvae display stereotypic episodes of forward peristalsis (straight move) and brief episodes of head swinging and turning [pause & turn, named 'Pause' in (e)]. In contrast, *scribbler* larvae spend most of their time in repetitive pause and turn episodes and backward moves. (b-e) Parameters of locomotion in sbb^3/CyO^{GFP} and homozygous sbb^3 mutant larvae. (b) The peak instantaneous speed (mm/second) is significantly reduced in sbb^3 mutant compared to sbb^3/CyO^{GFP} larvae. (c) Mean absolute turning rate (deg/second) is approx. three times higher in sbb^3 mutant compared to sbb^3/CyO^{GFP} larvae. (d) Mean duration of straight moves is significantly reduced in sbb^3 mutant larvae. (e) Mean duration of pause [pause and turn in (a)] episodes is ~10 times longer in sbb^3 mutant larvae. See *Materials and methods* for criteria used to define straight moves and pauses. Bars are mean ± SEM. *n* is indicated over the bars in (b). $***P < 0.0001$ (unpaired *t*-test). (f) Developmental profile of turning rate in homozygous mutant (sbb^3, open circles), heterozygous sibling sbb^3/CyO^{GFP} (control, black filled circles), and wild type *CS* (wt, grey filled circles). Movies of crawling were recorded at 24, 26, 31, 43, 52, 96 ± 2.5 and ~110 h of age (after hatching) for sbb^3 mutant and control, and independently at 24, 30, 48, 80 ± 1 and ~110 h for *CS* (wt). Each circle represents the mean ± SEM and $n = 10$ per time point. No differences in turning rate were detected at 24, 26 and 31 ± 2.5 h of age (sbb^3 vs. control, $P > 0.05$; unpaired *t*-test). A significant difference in turning was detected from 43 ± 2.5 h onwards (sbb^3 vs. control; $*P < 0.05$). A bar over the x-axis indicates the time window during which aberrant turning ensues in the mutant. (g) Conditional expression of *sbb3.6* in neurons alone by means of the drug-inducible progesterone receptor-GAL4/UAS (GeneSwitch) system. The turning rate (deg/second) was measured for sbb^3 mutant larvae expressing the *sbb3.6* transcript in all neurons under the control of the elav promoter (*C155-GAL4*; sbb^3/sbb^3; *UAS-sbb3.6*/+). *C155-GAL4* was used as a control (*C155-GAL4*). sbb^3/sbb^3; *elav-GeneSwitch/UAS-sbb3.6* larvae were fed the progesterone drug (RU486) from the time points indicated on the x axis (0, 24, 41, 54, 64 and 72 ± 2.5 h after hatching) and locomotion was tested at ~66 h (for larvae fed at 0 h) or ~96 h (for all the rest). In the absence of the drug (no induction), the turning defect is evident. Induction of *sbb* expression from 0, 24 and 41 h reduced turning rates (0, 24 or 41 h vs. no induction; $***P < 0.001$, unpaired *t*-test, dark bars) to levels indistinguishable from those of the control (0, 24 or 41 h vs. *C155-GAL4*, NS). In contrast, GeneSwitch induction from 54, 64 and 72 h onwards did not restore normal turning (54, 64 or 72 vs. *C155-GAL4*, $P < 0.001$ and $P > 0.05$ when compared to no induction, light bars). Bars are mean ± SEM. $n = 15$ for *C155-GAL4*, $n = 8$ for no induction and $n = 8$ for all others.

K-acetate filled glass microelectrodes (60–80 MΩ). To reliably evoke spontaneous firing of the motoneurons (Barclay *et al.* 2002), the preparation was slowly heated from room temperature (~22 °C) to 35 °C. Once at 35 °C, spontaneous EJPs were recorded for a similar period of time in both control and mutant larvae (control: 6 ± 1 min, $n = 10$ larvae vs. mutant: 4.8 ± 0.3 min, $n = 6$ larvae). Only recordings in which the resting membrane potential held stable were later analyzed (control: −66.3 ± 1.4 mV, $n = 10$ larvae; mutant: −62.9 ± 3.7 mV, $n = 6$ larvae, $P > 0.05$) (see *Results* and Fig. 6). An Axoclamp-2A (Axon Instruments, Inc. Union City, CA) amplifier recorded the membrane potential; the signal was low-pass filtered at 5 kHz to remove high frequency noise. Data were acquired to disk using a MacLab/4s data acquisition system (ADInstruments, Toronto, ON) and a Power PC Macintosh computer. The duration and frequency of EJP 'episodes' (*Results*), was obtained using functions available in CHART v3.5.4/s (Macintosh; ADInstruments). For analysis of intraburst EJP events (Fig. 6b, ii), AXOGRAPH 4.6 (Axon Instruments, Inc.) was used, and cumulative probability distributions of time intervals (ms) between consecutive EJPs plotted using IGOR PRO 3.16 (WaveMetrics, Inc.). Means were compared using the Student's *t*-test in SPSS, unless indicated otherwise. Standard error of the mean (SEM) is presented throughout the manuscript.

Results

To characterize the spontaneous pattern of locomotion in individual larvae on non-nutritive agar, we recorded 3-min episodes of crawling on a non-nutritive agar substrate using a 2D computer-assisted tracking system (Suster & Bate 2002). On this arena, non-mutant third instar larvae (96 ± 4 h after hatching) stereotypically alternate between long episodes of forward peristalsis (named straight moves) and brief episodes of head swinging and turning (named pauses) (Fig. 1a).

Larvae homozygous for the severely hypomorphic pupal-lethal sbb^3 mutation (*w*; sbb^3/sbb^3; *ry*), display striking changes in the pattern of locomotion compared to heterozygous siblings (*w*; sbb^3/CyO^{GFP}; *ry*). Mutant larvae engage in repetitive episodes of head swinging and turning and backward locomotion (Fig. 1a, sbb^3/sbb^3, *pause & turn* and *backward move*). Mutant larvae crawl on average more slowly (mean = 0.16 ± 0.01 mm/second vs. 0.35 ± 0.02 mm/second in control, $n > 15$, $P < 0.0001$), partly because of slower peristalsis, which is reflected by a reduction in the peak instantaneous speed (Fig. 1b). Episodes of forward peristalsis appear, qualitatively, largely unaffected in mutant larvae, but are frequently interrupted by head swinging and turning; hence mutant larvae show a high turning rate (Fig. 1c) and spend significantly less time in linear locomotion (Fig. 1d). In contrast, these larvae engage in excessively long pauses (Fig. 1e) during which they frequently turn at > 120 degree angles (frequency of > 120 deg turns = 8 ± 1.3 per min in mutant vs. 3 ± 0.9 in control, $n > 10$, $P < 0.01$). Although mutant larvae perform frequent head turns, they do not show a preference for turning in any particular direction (mean turning bias = − 0.83 ± 0.65 deg/second in control vs. −0.43 ± 0.77 deg/second in mutant, $n > 15$, $P > 0.05$) suggesting that, like wild type larvae, they are able to alternate head swings between either half of the body.

We examined the development of turning behavior in *sbb*^{3} hypomorphic mutant, control heterozygous (*sbb*^{3}/*CyO*^{GFP}) and wildtype *CS* larvae. *sbb*^{3}/*CyO*^{GFP} larvae show a stable turning rate throughout development like wild type larvae *CS* (Fig. 1f). Compared to controls, mutant larvae show no detectable defects in locomotion early in larval life (at 24, 26, 31 h each time period having a range of $\pm$ 2.5 h) (Fig. 1f). However, at the 43 $\pm$ 2.5 h time point, before the onset of the third instar which occurs around 48 h under the rearing conditions we used, we found a significant increase in turning in *sbb*^{3} mutant larvae compared to the controls. This increase in turning rate persisted until late larval life (~110 h posthatch) (Fig. 1f).

Given the onset of locomotor abnormalities in the *sbb*^{3} larvae, we asked whether the small *sbb* transcript is needed early in larval life for wild type locomotion. To address this, we took advantage of a conditional GAL4/UAS expression system (*GeneSwitch*) in which the DNA-binding domain of GAL4 is fused to the activation domain of the progesterone receptor (Osterwalder *et al*. 2001), and which can be conditionally activated by a progesterone analog (RU486) upon feeding. We targeted expression of the small *sbb* transcript using an *elav* driver because we had previously shown that it restored turning behavior to wild type levels (Yang *et al*. 2000). Specifically, we used an *elav-GeneSwitch* driver to selectively induce *sbb3.6* expression in neurons at various times of larval development using the *UAS-sbb3.6* transgene (Fig. 1g) in the *sbb*^{3} hypomorphic mutant background (*sbb*^{3}/*sbb*^{3}; *elav-GeneSwitch/UAS-sbb3.6* in Fig. 1g). We turned on the expression of the small *sbb* transcript at various time points during larval development (at 0, 24, 41, 54, 64 and 72 h of larval life). Turning rate was then measured in the late third larval instar (see *Materials and methods*). Note that the times in hours do not provide the precise age of the larva at which the *sbb* transgene is expressed because larval age is $\pm$ 2 h and more importantly GeneSwitch mediated-protein expression is normally detected 5 h after feeding of RU486 (Osterwalder *et al*. 2001) so the time estimates plotted on

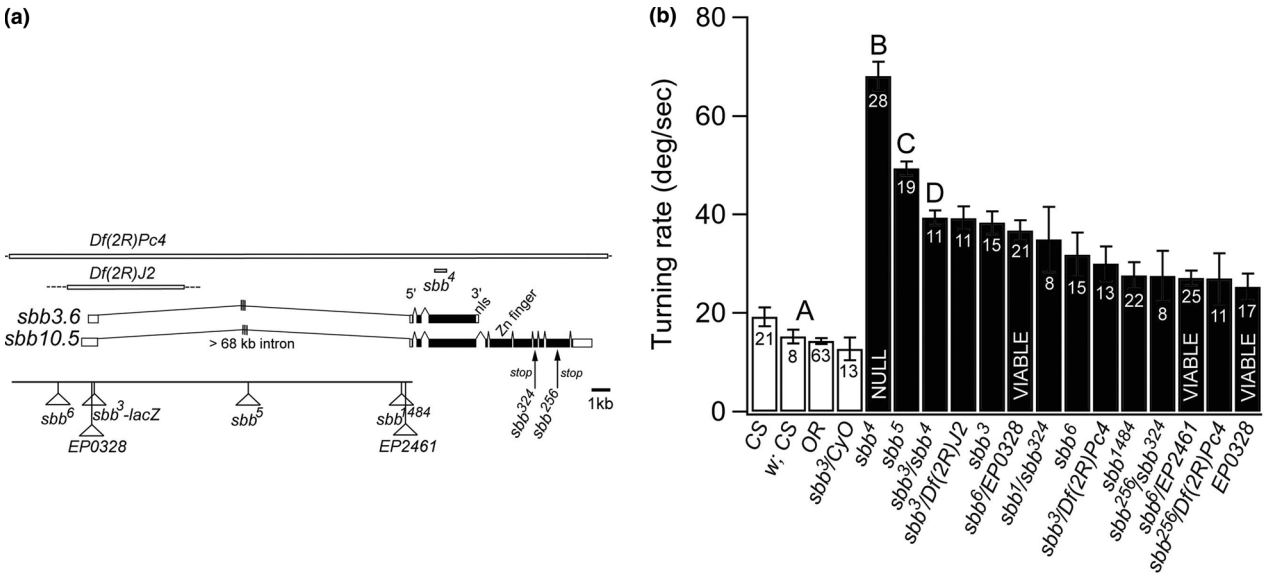

Figure 2: Aberrant turning in larvae from null, lethal and viable *scribbler* mutant alleles. (a) Schematic diagram of the *sbb* genomic region, illustrating *sbb* transcripts and mutations used in this study. Two predominant transcripts (3.6 kb long, *sbb3.6* and 10.5 kb long, *sbb10.5*) are generated from a large (> 80 kb) genomic region (from left to right, 5′ to 3′). The current study examines the function of the *sbb3.6* transcript. Coding exon (filled) and non-coding exons (unfilled) are drawn as rectangles, and introns represented by lines joining consecutive exons. (a) > 68 kb intron (hatched lines) splits the first non-coding exon. Both *sbb* transcripts include a nuclear localization signal (nls). The transcript not examined in this study is the *sbb10.5* that contains a single C2H2 type Zn^{+2} finger domain (Zn finger). Chromosome deletions are depicted as unfilled rectangles (top). Pupal-lethal and viable *P*-elements are shown as triangles and their approx. site of insertion indicated relative to each other (bottom left). Two point mutations (*sbb*^{256}, *sbb*^{324}) introduce stop codons in the *sbb10.5* transcript (arrows, stop) (see *Materials and methods* for more details). Aberrant turning in larvae from null, lethal and viable *scribbler* mutant alleles. (b) Mean turning rate (deg/second) was obtained for control (unfilled bars) and mutant (filled bars) larvae (110 $\pm$ 5 h after hatching) as described in Fig. 1. In wild type (*CS*, *OR*), *white* (*w; CS*), and control (*sbb*^{3}/*CyO*^{GFP}) larvae, mean turning rate ranges between 12 and 19 deg/second. Mutant alleles share the *w* background except for *Df(2R)Pc4*. Alleles are arranged from left to right in order of decreasing severity. Null larvae (*sbb*^{4}/*sbb*^{4}, NULL) show the most significant increase in turning rate. Viable alleles or allelic combinations are indicated over the appropriate bar (VIABLE); the remaining bars represent pupal-lethal alleles or allelic combinations. Bars are mean $\pm$ SEM. *n* is indicated over each bar. ANOVA ($F_{18,323} = 39.3$, $P < 0.0001$) and SNK ($P < 0.05$) revealed statistically significant differences in turning rate between control (unfilled bars) and mutant (filled bars) strains. Statistically different groups detected by SNK are labeled by letters A-D (D includes all non-labeled bars, and can be further subdivided into three largely overlapping groups).

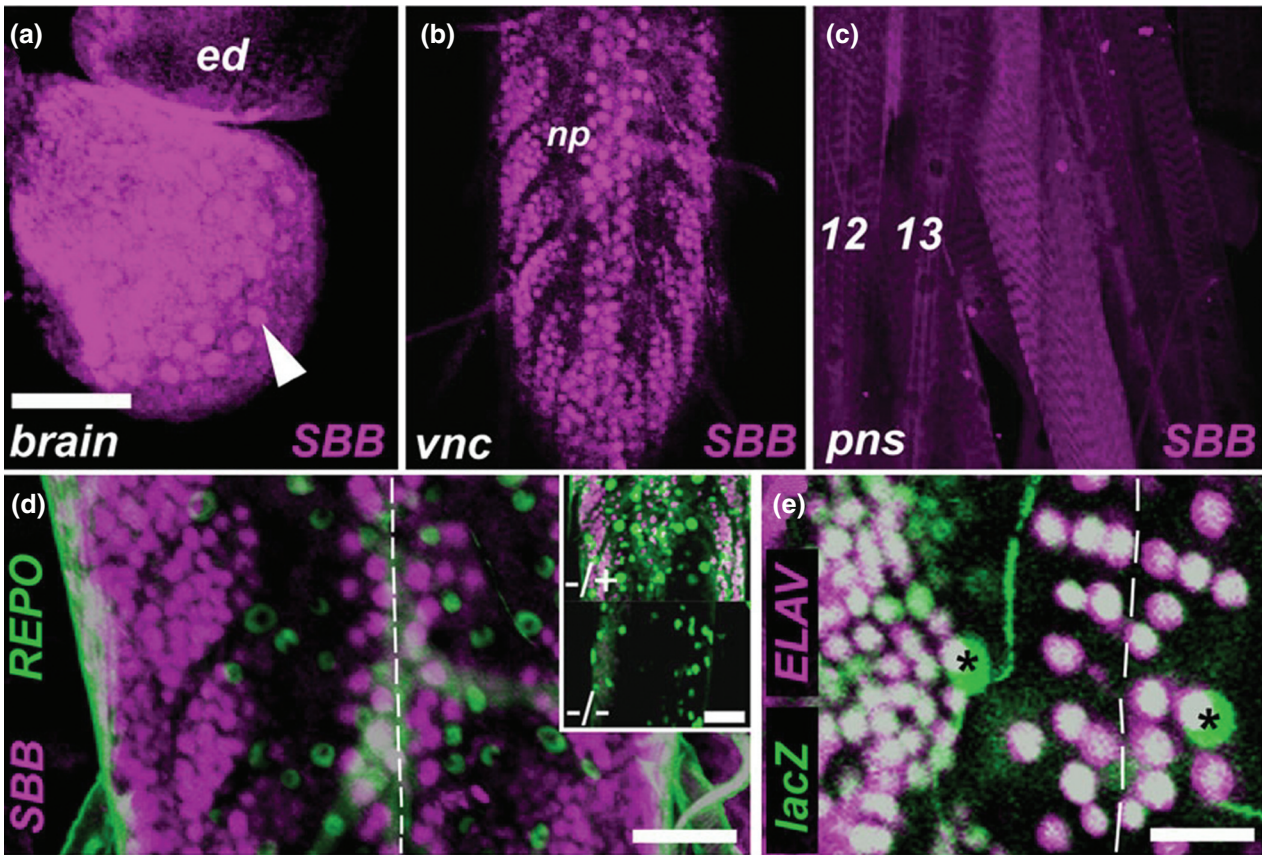

Figure 3: SBB is expressed in the nucleus of most, if not all, central neurons. Larval tissues were labeled with SBB (a-c), SBB and REPO (d) or β-gal and ELAV (e) antibodies. The wild type control (sbb^3/CyO^{GFP}) was used in (a-c) and (e). In (d) (inset), sbb^1/CyO^{GFP} (–/+) and sbb^1 null (–/–) larvae were used. In (e), the expression of the *lacZ* enhancer-trap in sbb^3 (Fig. 2a) was revealed. Images of the larval brain [brain in (a)], ventral nerve cord [vnc; full vnc in *B*, abdominal segments in (d-e)] or a body wall hemi-segment (c), were obtained by confocal microscopy (as in Fig. 4), and are shown here as 3D projections. Anterior is to the top. (a) SBB expression in the brain. One brain hemisphere is shown. The midline is to the left. Strong expression is detected in neuroblasts (arrowhead) and in most other cells. The adjacent eye disc (ed) also shows nuclear staining. (b) SBB is strongly expressed widely in the nuclei of most cells in the vnc. The neuropile (np) is indicated on the left half of the vnc. (c) SBB expression was not detected in the body wall, including the cells of the peripheral nervous system (pns) or musculature. Muscle 12 and 13 are labeled for reference. The midline is to the right. (d) SBB-labeled nuclei (magenta) do not express the glial marker REPO (green). The midline is indicated by a stippled line. Scale bar = 50 μm. Inset shows SBB and REPO double labeling of the VNC in sbb^1 null (–/–) and heterozygous control (–/+) larvae. SBB staining is absent in the null. Scale bar = 44 μm. (e) sbb^3-*lacZ* labeled nuclei (green) coexpress the neuronal marker ELAV (magenta). The midline is indicated by a stippled line. Every cell adjacent to the dorsal midline coexpresses *lacZ* and ELAV (white). Scale bar = 25 μm. Asterisks indicate cells labeled by *lacZ* only [i.e. not labeled by the SBB antibody in (b)].

the *X*-axis of Fig. 1g should be considered in this context. Overall the results show that inducing *sbb* expression in the larval CNS early in life (before the third instar) restores turning behavior to a wild type level whereas inducing *sbb* expression later in larval life (in the third instar) does not. This loosely parallels the timing of the onset of turning behavior shown in Fig. 1f. Together these data suggest that *sbb* acts in neurons during early larval life (prior to the third instar) for normal turning behavior.

We measured turning rate in a variety of *sbb* mutant lines including null, hypomorphic, lethal and viable *sbb* mutant alleles (Fig. 2a). Two main observations were derived from our analysis of *sbb* alleles. First, larvae from viable mutant alleles (see bars labeled *VIABLE* in Fig. 2b), whose external and internal morphology appear indistinguishable from wild type, manifest defects in larval turning rate that are as severe as those of larvae from lethal alleles (compare viable sbb^6/*EP0328* to pupal-lethal homozygous sbb^6 in Fig. 2b). This indicates that locomotor defects in *sbb* mutant larvae can occur independently of pupal or late larval lethality. Secondly, several heterozygous mutant combinations using sbb^1, which is a protein null with mutations that affect the large

(10.5 kb) transcript but not the small (3.6 kb) *sbb* one [sbb^1/sbb^{324}, sbb^{256}/sbb^{324} and sbb^{256}/*Df(2R)Pc4*], result in a significant increase in turning rates (Fig. 2b). This suggests that the large transcript plays a role in larval turning behavior. It is not possible to obtain mutants that only disrupt the small transcript because the small transcript is a subset of the large one. It will be of interest to examine turning rates in null larvae with transgenes made from the small, large or the small and large transcripts together.

We next examined the distribution of SBB proteins in embryonic and larval tissues. We used two antibodies raised independently against peptide sequences common to both SBB proteins (Rao *et al.* 2000; Senti *et al.* 2000). Similar results were obtained with both antibodies and neither produced staining in sbb^1 or sbb^4 null larvae (inset in Fig. 3d and data not shown). In embryos, SBB is expressed ubiquitously and restricted to nuclei from the earliest stages of development. By late embryonic stages, SBB becomes highly enriched in the nervous system (data not shown).

After embryonic hatching, SBB expression remains strong in the larval CNS (Fig. 3a,b), and can be detected in neuroblasts (arrowhead in Fig. 3a), neurons and in the proliferating or differentiating cells of the eye imaginal disc (ed in Fig. 3a). SBB was largely undetected in the nuclei of the peripheral nervous system (PNS), larval body wall or in the musculature (Fig. 3c). To confirm the identity of the cells that express SBB, we double labeled the larval CNS with antibodies against SBB and REPO (a glial nuclear marker), and separately with a *lacZ* enhancer-trap in sbb^3 (whose expression can be detected with a β-gal antibody) and an ELAV antibody (a marker for differentiated neurons). SBB positive cells did not coexpress REPO (Fig. 3d) indicating that SBB expression

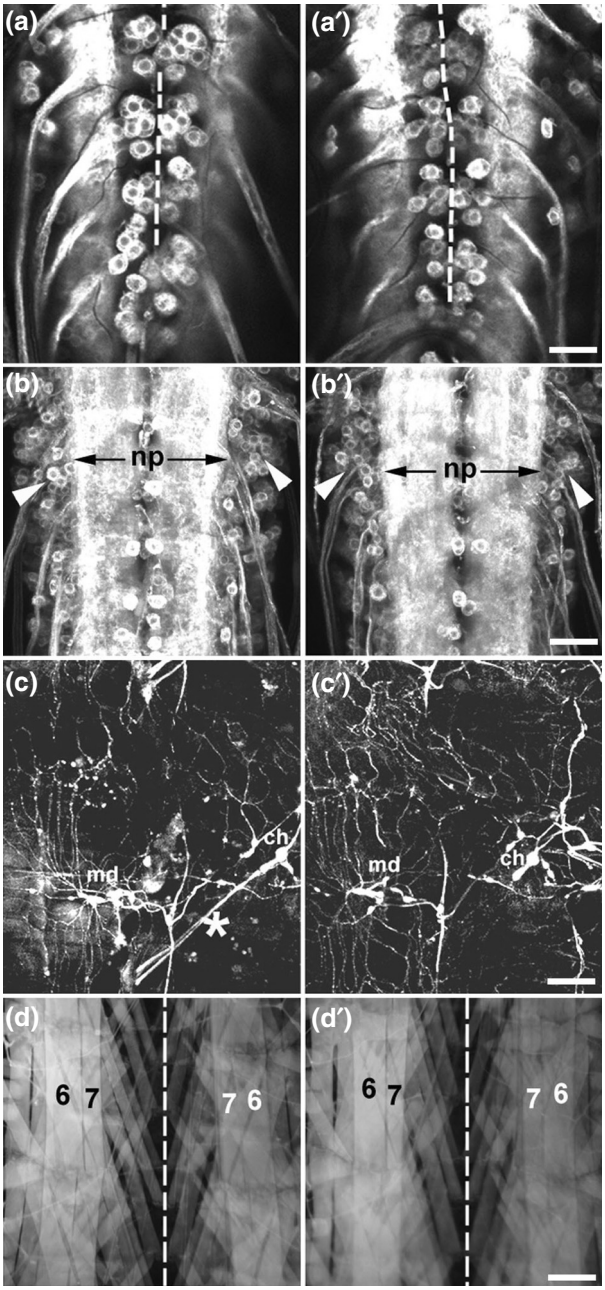

Figure 4: *scribbler* mutant larvae do not display any obvious gross morphological defects of the nervous system or musculature. Dendritic and axonal projection patterns are not shown. Motoneurons, cholinergic neurons or muscles were visualized in the sbb^3/CyO^{GFP} (a-d) or sbb^3/*Df(2R)J2* mutant (a′-d′) background by GAL4-driven expression of a mouse CD8 and GFP fusion protein. sbb^3/CyO^{GFP} flies carrying the appropriate GAL4 driver were crossed to sbb^3/*Df(2R)J2*; *UAS-mCD8-GFP*. GFP fluorescence was imaged under a laser confocal microscope (a,a′-c,c′) or a light microscope equipped with GFP fluorescence filters (d,d′). Images are 3D projections (of identical thickness for each pair), except for those in a,a′ and d,d′ which are optical sections. Anterior is to the top. Comparable segments are shown in the abdominal VNC (a-b′) or body wall (c-d′). (a,a′) Motoneurons on the dorsal surface of the VNC labeled by the *OK6-GAL4* driver. The midline is indicated by a stippled line. GFP-labeled cell bodies are located on either side of the midline. Motor axons exit from the edges of the VNC. Scale bar = 25 μm. (b,b′) Central cholinergic neurons labeled by the *cha-GAL4* driver. The lateral edges of the neuropile (np) are indicated by arrows. Cell bodies are adjacent and lateral to the neuropile (arrowheads). Scale bar = 20 μm. (c,c′) Cholinergic sensory neurons in the larval body wall labeled by the *cha-GAL4* driver. Comparable multidendritic neurons (md) and lateral chordotonal organs (ch) are shown. The asterisk near the ch organ in (c) points to GFP-labeled material from the *actin-GFP* transgene of the CyO^{GFP} balancer. Scale bar = 110 μm. (d,d′) Ventral and lateral body wall musculature. The midline is indicated by a stippled line, and muscles 6 and 7 are labeled for reference. Scale bar = 120 μm. No consistent differences were observed between mutant and control samples ($n = 10$ each).

is not glial. We found that all cells labeled by *sbb*^{3}-*lacZ* (β-gal positive) were also labeled by the ELAV antibody (Fig. 3e). Thus we found SBB to be expressed in neurons of the CNS.

Immunostaining with an extensive panel of antibodies that label the central and/or peripheral axonal scaffold (e.g. 22C10, FASII, ChAT), all neurons (e.g. ELAV), glia (e.g. REPO), subsets of motoneurons (e.g. EVE) or interneurons (e.g. FMRFamide, ACJ6, TH, PHM), revealed no visible defects in the mutant nervous systems of *sbb*^{3}/*sbb*^{3} and *sbb*^{3}/*Df(2R)J2* mutant embryos and wandering larvae (~110 h). We found that homozygous larvae with severe mutant alleles (e.g. *sbb*^{1}, *sbb*^{3} or *sbb*^{4}) had smaller central nervous system (CNS) presenting us with an interesting observation for future study. Mutant larvae with several heteroallelic pupal lethal combinations (e.g. *sbb*^{3}/*Df*(*2R*)*J2*, *sbb*^{6}/*EP0328*, *sbb*^{324}/*sbb*^{4}, *sbb*^{256}/*Df*(*2R*)*Pc4*) and those with viable alleles (e.g. *EP0328*, *EP2461*) appeared to have no visible defects in their nervous systems (Fig. 4 and data not shown) at the level that we examined their morphology.

To examine the processes of neurons or glia in the mutant nervous system, we used the GAL4/UAS system (Brand & Perrimon 1993). In this system, expression of the yeast transcriptional activator GAL4 is driven by a selected enhancer that in turn activates the expression of a chosen transgene through the upstream activating sequence (UAS). A membrane-targeted fusion of the mouse CD8 antigen and GFP (CD8-GFP) was expressed in defined cell types using several GAL4 drivers in the *sbb*^{3}/*Df(2R)J2* mutant background. Targeted expression of CD8-GFP in all neurons with the pan-neural *C155-GAL4* (sometimes referred to as *elav-GAL4*) driver, or in glia with the *repo-GAL4* driver, revealed no obvious abnormalities in the organization of conspicuous neuropile structures (e.g, mushroom bodies), in the arrangement of cell bodies or neuropile in the ventral nerve cord (VNC), in the peripheral projections of motoneurons or in the processes of glia within the CNS (data not shown).

GFP-labeled motoneurons in control (*sbb*^{3}/*CyO*^{GFP}) and mutant (*sbb*^{3}/*Df*(*2R*)*J2*) wandering larvae appeared indistinguishable (cell bodies on either side of *stippled line* in Fig. 4a). The cell bodies and axonal processes of central and peripheral cholinergic neurons labeled by GFP (using the *cha-GAL4* driver) did not display visible abnormalities in mutant larvae (Fig. 4b,c, respectively). The size and morphology of individual muscles labeled by *24B-GAL4*-driven GFP expression appeared unaltered in mutant larvae Fig. 4d. We also examined the morphology of GFP-labeled peptidergic, dopaminergic, serotonergic and other interneurons (using the *c929-GAL4*, *386Y-GAL4* and *Ddc-GAL4* drivers) and did not detect any visible defects (data not shown). Thus with currently available cellular markers and at the level of our analysis we were unable to detect visible defects that correlate with the aberrant locomotion of *sbb* mutant larvae.

As *sbb* is expressed in most, if not all, central neurons and neuroblasts, it is possible that *sbb* is required in widely distributed and diverse sets of cells in the nervous system for normal turning behavior. To identify the minimal set of cells in which the small *sbb* transcript is sufficient for wild type behavior, we used the binary GAL4/UAS expression system. First, we confirmed that leaky expression of *sbb3.6* under a heat shock promoter (no heat shock applied; Yang *et al.* 2000), in the *sbb*^{3} mutant background, is sufficient to restore wild type locomotion (*sbb*^{3}; *hs-sbb3.6* in Fig. 5a). Secondly, we used 25 tissue-specific GAL4 lines to drive expression of *sbb3.6* in defined sets of neurons or in other cell types in the *sbb*^{3} mutant background (*sbb*^{3}/*sbb*^{3}*: GAL4: UAS-sbb3.6* in Fig. 5a).

We verified that all of the GAL4 drivers used in our study (Fig. 5a) can drive strong and consistent UAS-linked transgenic expression (both nuclear and cytoplasmic expression) in the nervous system and musculature (using confocal microscopy, examples shown in Fig. 5b). GAL4 lines expressed in the nervous system were also crossed to UAS-linked tetanus toxin transgenes producing consistent behavioral phenotypes that confirmed their neural expression (Suster *et al.* 2003). We assume that the UAS-*sbb3.6* transgene used in Figs 1 & 5a generates a functional SBB protein because GAL4-driven expression from this transgene is capable of restoring larval behavior, pupal lethality and all other defects associated with loss of SBB in all *sbb* mutants, including the *sbb*^{4} null allele.

We first confirmed that the small *sbb* transcript is needed in differentiated neurons for normal turning behavior (Yang *et al.* 2000) and then went on to ask whether it was needed in neuronal precursors (neuroblasts), early born neurons or non-neuronal cell types to restore normal turning behavior. We found that the expression of *sbb* in all differentiated neurons with the pan-neural *C155-GAL4* driver or with the *cha-GAL4* driver was sufficient to fully restore wild type behavior (Fig. 5a). Targeted expression of *sbb* in all neuroblasts and their immediate progeny with the *Mz1060-GAL4* (Fig. 5b) or *l(3)-31-GAL4* drivers did not restore wild type locomotion (bar labeled *neuroblasts* in Fig. 5a). Expression of *sbb* in all glia driven by *repo-GAL4*, in a subset of glia driven by *Mz840-GAL4*, in embryonic and/or larval musculature with *24B-GAL4* (which also labels mesoderm and trachea) and *Nrv1-GAL4* or *Mhc-GAL4*, in epidermis and imaginal discs with *hh-GAL4*, in gut and secretory cells with *c929-GAL4* and *386Y-GAL4* did not restore wild type locomotion (Fig. 5a). We infer from these results that the small *sbb* transcript is uniquely required in differentiated neurons, and that expression in neurons targeted by the *cha*-GAL4 driver also restores wild type turning behavior.

As the *cha*-GAL4 driver comprises both central neurons and peripheral sensory neurons in *Drosophila* (Salvaterra & Kitamoto 2001) (Figs 4b,c & 5b) we asked whether targeting the small *sbb* transcript to sensory neurons alone would restore normal turning behavior. However, targeted expression of this transcript in all embryonic and early larval sensory neurons with the *P0163-GAL4* driver, in all embryonic and

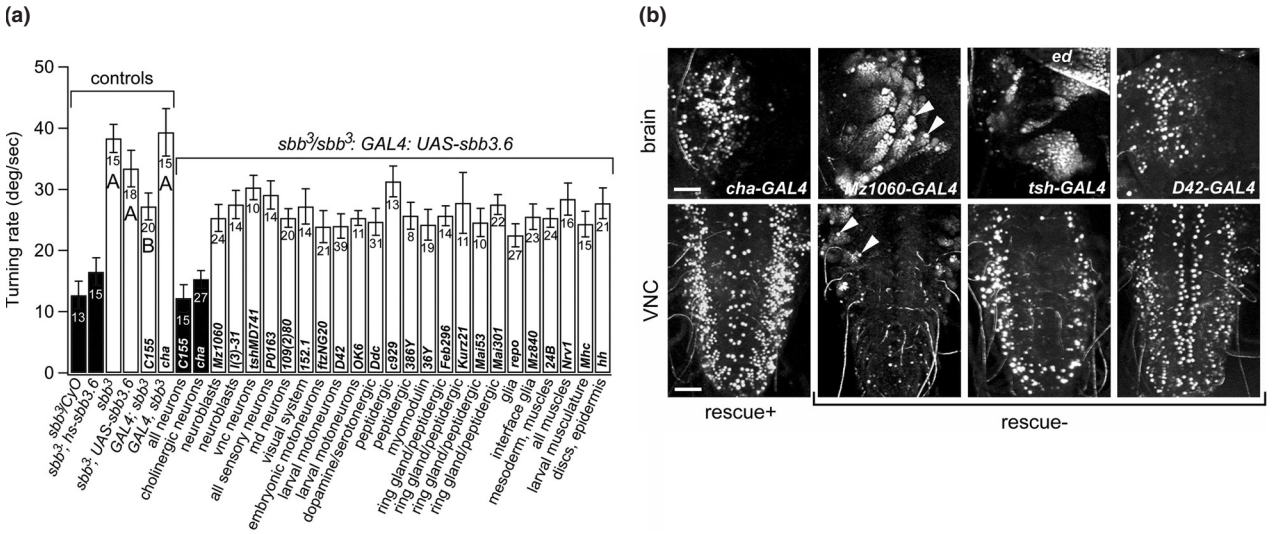

Figure 5: Targeted expression of the *sbb3.6* transcript in differentiating neurons (C155-GAL4) or in the *cha-GAL4* pattern was sufficient to rescue the aberrant turning rates of sbb^3/sbb^3 hypomorphic mutant larvae. Flies carrying a GAL4 driver in the sbb^3 mutant background were crossed to flies carrying a *UAS-sbb3.6* transgene in the same background (*sbb10.5* was not used for rescue experiments in the present study). Movies of crawling (~110 h old larvae) were recorded for 3 min and turning rate (deg/second) obtained as in Fig. 2. (a) Mean turning rate in larvae from controls and from GAL4 crosses (sbb^3/sbb^3: *GAL4*: *UAS-sbb3.6*). Ubiquitous expression of the 3.6 kb transcript driven by a 'leaky' heat shock promoter fully restored wild type turning (sbb^3; *hs-sbb 3.6* vs. sbb^3/CyO^{GFP} control). The *UAS-sbb3.6* transgene alone did not rescue aberrant turning (sbb^3; *UAS-sbb3.6* vs. sbb^3/sbb^3). GAL4 lines are indicated over each bar on the graph, and a brief description of the cell types in which GAL4 is expressed is provided under the *X* axis (see *Results and Materials and methods* for more details). The *C155-GAL4* enhancer-trap alone caused a small but significant suppression of turning (*GAL4;* sbb^3 vs. sbb^3/sbb^3); all other GAL4 lines had a similar effect on turning (unfilled bars). The *cha*-GAL4 driver alone did not suppress the aberrant turning of sbb^3 (*GAL4*, sbb^3; bar labeled *cha*). Expression of *sbb* in *all neurons* (*C155*) or with the *cha-GAL4* driver fully rescued aberrant turning (filled bars). None of the other GAL4 lines restored turning rates to wild type levels (unfilled bars). Bars are mean ± SEM. *n* is indicated over each bar. ANOVA ($F_{30,528} = 5.7$, $P < 0.0001$) and SNK ($P < 0.05$) revealed statistically significant differences between the means of two large groups (filled bars and unfilled bars). The unfilled bars can be further subdivided into four overlapping SNK groups. Mutant controls (unfilled bars) are composed of 2 statistically different groups (A and B). (b) Larval expression pattern of *cha-GAL4*, a line that rescued aberrant locomotion (rescue+) and examples of three GAL4 lines that did not (rescue–). Larvae were obtained from crosses of *cha-GAL4*, *Mz1060-GAL4*, *tsh-GAL4*^{MD741}, or *D42-GAL4* to *UAS-GFP-nlacZ*. Confocal 3D projections of GFP-labeled brain hemispheres (top panel, brain) and ventral nerve cords (bottom panel, VNC) obtained as in Fig. 4. *cha-GAL4* labels a large number of neurons in the brain and VNC. *Mz1060-GAL4* labels most (if not all) neuroblasts (arrowheads) and adjacent neuronal progeny. *tsh-GAL4*^{MD741} labels a large number of cells in the brain, eye disc (ed) and a large subset of interneurons in the VNC. *D42-GAL4* labels a similar number of neurons to that of *cha-GAL4* in the brain and many other neurons in the VNC, including most (if not all) motoneurons. Scale bars = 50 μm.

larval multidendritic (md) neurons and a subset of chordotonal organs with *109(2)80-GAL4* or in the embryonic and developing adult visual system with *152.1-GAL4* and multiple other drivers (e.g. *hh-GAL4*, *Kurz21-GAL4*) did not restore wild type locomotion (bars labeled *all sensory neurons*, *md neurons*, *visual system* in Fig. 5a). This suggests that expression of the small *sbb* transcript in sensory neurons alone is not sufficient to restore wild type behavior. This indicates that *sbb* may be required in the central neurons targeted by the *cha-GAL4* driver.

Expression of the small *sbb* transcript in all embryonic and larval motoneurons with three independent drivers, *ftz-GAL4*, *D42-GAL4* and *OK6-GAL4*, did not restore wild type behavior (bars labeled *embryonic motoneurons* and *larval motoneurons* in Fig. 5a). This indicated that this transcript is not sufficient in motoneurons to rescue aberrant turning behavior. Expression of *sbb* in large subsets of interneurons, including dopaminergic and serotonergic neurons driven by the *Ddc-GAL4* driver or in ring gland and peptidergic interneurons with the *c929-GAL4*, *386Y-GAL4*, *36Y-GAL4*, *Feb-296-GAL4*, *Kurz21-GAL4*, *Mai53-GAL4* and *Mai301-GAL4* drivers, did not rescue aberrant turning behavior (Fig. 5a). Expression of *sbb* in a large set of VNC interneurons driven by the *tsh-GAL4*^{MD741} line (Fig. 5b) did not rescue the aberrant locomotor patterns either (bar labeled *vnc neurons* in Fig. 5a), supporting the hypothesis that expression of the small *sbb* transcript in large and widely distributed populations of neurons is not sufficient for wild type turning behavior. Taken together these results indicate that the small *sbb* transcript may be required in central cholinergic neurons for larval locomotion. Expression of the small *sbb* transcript in motoneurons was not sufficient to restore wild type locomo-

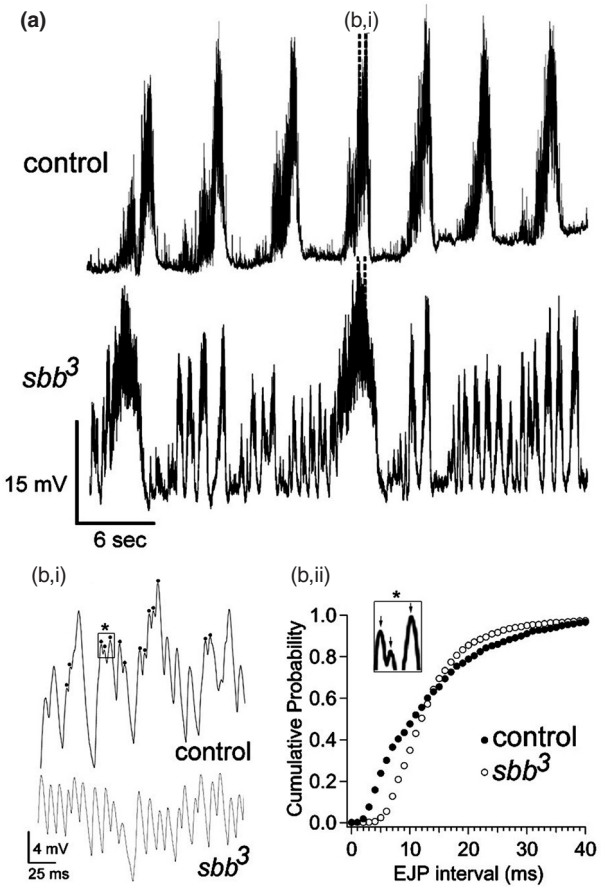

Figure 6: *scribbler* mutant larvae display alterations in spontaneous motoneuron activity patterns. Excitatory junction potentials (EJPs) were recorded from muscle fiber 6 in segments 2 or 3 with an intracellular electrode at ~35 °C. (a) Representative EJP activity from sbb^3/sbb^3; *hs-sbb3.6* (control) which rescues aberrant turning behavior and mutant (sbb^3) larvae. In general, muscle 6 manifests a rhythmic pattern of EJP 'bursts' (7 bursts in the control trace). The sbb^3 mutant trace shows a significantly more erratic pattern and more frequent activity episodes (see *Results* for parameters). Small sections (stippled lines) of EJP episodes of comparable amplitude are expanded in (b, i). (b) Intraburst EJP activity. (b, i) Section of the burst indicated in (a) expanded from control and sbb^3 mutant traces to illustrate the intraburst EJP frequency. Dots above the control denote EJPs that occur within 5–10 ms of an adjacent EJP (100–200 Hz activity). In sbb^3, EJPs occur at a more regular and different frequency to control. (b, ii) Cumulative probability distribution of EJP time intervals within 'bursts' ($n > 1000$ events per distribution, $N = 5$ bursts) in control and sbb^3. The distribution of time intervals in sbb^3 is significantly different from that of the control (Kolmogorov-Smirnov test, $Z = 4.3$, $P < 0.0001$).

tion. Furthermore, these transgenic rescue experiments suggest that this transcript is likely needed in a subset of the *cha*-GAL4 expression pattern, as the expression of *sbb* in all sensory neurons, or in widely distributed populations of interneurons did not restore wild type behavior.

Previous work from our lab (Yang *et al*. 2000) showed that targeted expression of the small *sbb* transcript to the nervous system alone using an *elav* driver restored normal turning behavior. To determine whether or not *sbb* mutants displayed a physiological phenotype, we assayed centrally generated bursts of electrical activity that are manifested in the musculature and are associated with larval peristaltsis (Barclay *et al*. 2002; Cattaert & Birman 2001).

Such activity can be monitored by recording excitatory junction potentials (EJPs) from a well-characterized longitudinal muscle fiber, abdominal muscle 6 (Keshishian *et al*. 1996) in the semi-intact larva (see *Materials and methods*). Muscle 6 receives innervation from two motoneurons (MN6/7-Ib and MSNb/d-Is in Hoang & Chiba 2001). We obtained intracellular recordings from muscle 6 in mutant (sbb^3/sbb^3) larvae and in control larvae of the same genotype expressing the *sbb3.6* transcript ubiquitously (sbb^3/sbb^3; *hs-sbb3.6*). Rhythmic EJP bursts were commonly observed in control larvae (Fig. 6a; $n = 10$ of 12 preparations) and were consistent with those of the wild type (Barclay *et al*. 2002). Interestingly, we found changes in the frequency and regularity of EJP activity in sbb^3 mutant larvae (Fig. 6a).

Mutant larvae displayed an irregular pattern of EJP activity. As a result, it was difficult to measure 'bursts' of rhythmic activity in an unambiguous way so we measured the frequency and duration of any 'episodes' of activity comprising at least 2 consecutive EJPs within 100 ms. Using this criterion, we detected more frequent and variable EJP episodes in mutant (20 ± 4.9 episodes/min, $n = 508$) compared to control larvae (10 ± 1.6 episodes/min, $n = 401$, $P < 0.05$). The average duration of EJP episodes was significantly shorter in mutant larvae (1.82 ± 0.08 seconds vs. 2.61 ± 0.11 seconds in control, $P < 0.001$). Thus it appears that under our recording conditions, motoneurons innervating muscle 6 in *sbb* mutant larvae manifest more frequent but briefer episodes of electrical activity. As the frequency of EJP episodes in control larvae (10 ± 1.6 episodes/min) is almost identical to the frequency of peristaltic waves in the intact but restrained wild type larva (7.2 ± 0.3 waves/min, $n = 10$ larvae, 87 observations), we suspect that on average every EJP 'episode' corresponds to an individual wave of peristalsis (see also Barclay *et al*. 2002; Cattaert & Birman 2001). The more frequent and shorter EJP episodes of mutant larvae, however, likely represent subthreshold events that fail to generate muscle contractions sufficiently sustained or powerful for peristalsis. This claim is supported by the observation that intact, but restrained, mutant larvae manifest significantly fewer peristaltic waves per unit time (3.7 ± 0.3 waves/min, $n = 6$ larvae, 30 min observation) compared to wild type larvae (7.2 ± 0.3 waves/min, $n = 10$ larvae, 87 min observation, $P < 0.0001$).

To examine the activity of motoneurons that could be relevant to muscle contractions during locomotion, we plotted the cumulative probability distribution of time intervals between consecutive EJPs (Fig. 6b, ii) within 'bursts' of

high frequency activity (e.g. parallel dotted lines in Fig. 6a, expanded in 6b, i). EJPs in the control occur 5 and 10 ms apart (Fig. 6b, i&ii). These intervals correspond to firing frequencies in the range of 100–200 Hz consistent with a previous report of 100 Hz instantaneous firing in the wild type (Barclay *et al.* 2002). In mutant larvae, we observe a more regular pattern of EJPs that occur often 10–15 ms apart, corresponding to firing frequencies of ~70–100 Hz (Fig. 6b, i&ii). Motoneurons in *sbb* mutant larvae may still manifest firing frequencies of 100 Hz or greater (EJP intervals ≤ 10 ms in Fig. 6b, ii) indicating that the motor axons and neuromuscular junctions (NMJs) in these animals are capable of transducing high frequency activity.

Our data suggest that the pattern of motoneuron activity in *sbb* mutant larvae is aberrant in both the number of 'bursts' generated per unit time, and the duration of these 'bursts'. The altered pattern of EJP activity in mutant larvae suggests that motoneurons may not receive the appropriate electrical input. In vertebrates, premotor interneurons regulate the firing frequency of spinal motoneurons (Binder & Powers 2001; Sillar & Roberts 1993; Wolf & Roberts 1995) so it is possible that defects in interneuron function could underlie the aberrant spontaneous activity of *sbb* mutant motoneurons. Future experiments will determine whether the *sbb* physiological phenotype described here is in any way related to the behavior of *sbb* mutant larvae.

Discussion

Most animals, including humans, manifest characteristic motor behaviors during development (Forssberg 1999; Sanes *et al.* 2000). For instance, frogs and zebrafish display stereotypic coiling and swimming movements as early as embryonic life. While much is known regarding the neurophysiological mechanisms of locomotion (reviewed in Grillner *et al.* 2000; Marder & Bucher 2001), the mechanisms by which genes control the development and organization of motor behavior and the underlying neural circuitry remain largely unknown. Here we have shown that the *Drosophila* larva provides a valuable model to identify genes required for locomotor behavior.

Despite the increased turning rate found in *scribbler* mutant larvae, this aberrant locomotion does not appear to be due to visible defects of the nervous system or musculature at the level of our measurements (Fig. 4). However, some *sbb* mutations cause obvious defects in photoreceptor (PR) axon targeting in the developing adult visual system (Rao *et al.* 2000; Senti *et al.* 2000). Defects in developing PRs are unlikely to account for the aberrant turning of *sbb* mutant larvae, because ablation of all PRs in pGMR-*hid* larvae (Busto *et al.* 1999) does not disrupt the spontaneous pattern of larval locomotion (mean turning rate $= 10.5 \pm 2.2$ deg/second in pGMR-*hid* vs. 13.5 ± 1.8 deg/second in *CS*, $n = 8$, $P > 0.05$). However, the axonal projections of a small set of CNS neurons that we were unable to examine may be affected in *sbb* mutant larvae.

In both vertebrates and invertebrates, locomotion depends on sensory input that provides critical feedback to circuitry in the CNS (Pearson 1995). *Drosophila* larvae lacking sensory input show reductions in crawling speed and a pronounced increase in turning rates (Suster & Bate 2002). These defects are similar to those of *scribbler* mutant larvae (Fig. 1). However, we found that *sbb* is not required in sensory neurons for wild type locomotion (Fig. 5). Our rescue experiments using *cha-GAL4* and other drivers suggest that the increased turning rate found in *sbb* mutant larvae may arise from defects in more central cholinergic neurons. We found that in the larva, SBB appears to be expressed in central rather peripheral sensory neurons (Fig. 3) and expression of *sbb* in sensory neurons is insufficient to restore wild type locomotion (Fig. 5). These findings, together with the fact that *sbb* is rescued using the *cha*-GAL4 driver but not using motoneuron drivers raise the hypothesis that *sbb* may be required in cholinergic interneurons for wild type behavior. However, this needs further verification using independent approaches. Pharmacological and physiological experiments could be used to determine whether *sbb* plays a restricted role in the specification of cholinergic neurons or whether it acts more broadly to specify a small but heterogeneous subset of central neurons that are labeled by *cha*-GAL4.

Recent electrophysiological studies indicate that embryonic and larval motoneurons in *Drosophila* receive rhythmic synaptic input from cholinergic interneurons (Baines *et al.* 2002; Rohrbough & Broadie 2002). Application of cholinergic antagonists or selective blockade of cholinergic transmission by expression of tetanus toxin light chain (TeTxLC; Sweeney *et al.* 1995), blocks synaptic input to motoneurons and larval peristalsis (Baines & Bate 1998; Baines *et al.* 2002). Bathing the semi-intact larva with Oxotremorine, an agonist of muscarinic cholinergic receptors, can evoke a fictive peristaltic rhythm by acting on the isolated VNC (Cattaert & Birman 2001). Interestingly, partial suppression of electrical activity in all cholinergic neurons by expression of a non-inactivating form of the *Shaker* K^+ channel (*EKO*; White *et al.* 2001), causes a reduction in speed and an increase in turning, consistent with those of *scribbler* mutant larvae (mean turning $= 54.4 \pm 5.2$ deg/second in *cha-GAL4/UAS-EKO* vs. 8.3 ± 2 deg/second in control, $P < 0.0001$). In contrast, blockade of synaptic activity in other sets of neurons (e.g, the Acj6 neurons, known to include > 500 interneurons, Certel *et al.* 2000) does not cause the turning defects observed in *sbb* mutant larvae (Suster *et al.* 2003). These observations support the proposed role of neurons targeted by *cha*-GAL4 in larval crawling in *Drosophila*, and the hypothesis that the aberrant behavior of *sbb* mutant larvae may in the future be related to defects in the electrical activity or synaptic properties of these neurons.

In the future, it will be of interest to determine whether the large scribbler transcript plays a role in turning behavior and if so whether the two transcripts function together to affect this behavior. The identification of the minimal subset of neurons in which the large and small *sbb* transcripts are required will

further aid in understanding its function in behavior. It should be possible to identify systematically the molecular targets, transcriptional partners and regulators of *scribbler* in these neurons using molecular and genetic interaction screens. Finally, it will be of interest to determine whether homologues of SBB in vertebrates (which show > 70% amino acid identity) function locomotion related behaviors.

References

Aberle, H., Haghighi, A.P., Fetter, R.D., McCabe, B.D., Magalhaes, T.R. & Goodman, C.S. (2002) Wishful thinking encodes a BMP type II receptor that regulates synaptic growth in *Drosophila*. *Neuron* **14**, 545–558.

Ashburner, M. (1989) *Drosophila. A Laboratory Manual*. Cold Spring Harbor Press, Cold Spring Harbor, NY.

Baines, R.A. & Bate, M. (1998) Electrophysiological development of central neurons in the *Drosophila* embryo. *J Neurosci* **18**, 4673–4683.

Baines, R.A., Seugnet, L., Thompson, A., Salvaterra, P.M. & Bate, M. (2002) Regulation of synaptic connectivity: levels of Fasciclin II influence synaptic growth in the *Drosophila* CNS. *J Neurosci* **22**, 6587–6595.

Barclay, J.W., Atwood, H.L. & Robertson, R.M. (2002) Impairment of central pattern generation in *Drosophila* cysteine string protein mutants. *J Comp Physiol A* **188**, 71–78.

Bate, M. (1999) Development of motor behavior. *Curr Opin Neurobiol* **9**, 670–675.

Berrigan, D. & Pepin, D.J. (1995) How maggots move: allometry and kinematics of crawling in larval diptera. *J Insect Physiol* **41**, 329–337.

Binder, M.D. & Powers, R.K. (2001) Relationship between simulated common synaptic input and discharge synchrony in cat spinal motoneurons. *J Neurophysiol* **86**, 2266–2275.

Brand, A.H. & Perrimon, N. (1993) Targeted gene expression as a means of altering cell fates and generating dominant phenotypes. *Development* **118**, 401–415.

Busto, M., Iyengar, B. & Campos, A.R. (1999) Genetic dissection of behavior: modulation of locomotion by light in the *Drosophila melanogaster* larva requires genetically distinct visual functions. *J Neurosci* **19**, 3337–3344.

Calleja, M., Moreno, E., Pelaz, S. & Morata, G. (1996) Visualization of gene expression in living adult *Drosophila*. *Science* **274**, 252–255.

Cattaert, D. & Birman, S. (2001) Blockade of the central pattern generator of locomotor rhythm by noncompetitive NMDA receptor antagonists in *Drosophila* larvae. *J Neurobiol* **48**, 58–73.

Certel, S.J., Clyne, P.J., Carlson, J.R. & Johnson, W.A. (2000) Regulation of central neuron synaptic targeting by the *Drosophila* POU protein, Acj6. *Development* **127**, 2395–2405.

Fetcho, J.R. & Liu, K.S. (1998) Zebrafish as a model system for studying neuronal circuits and behavior. *Annu N Y Acad Sci* **860**, 333–345.

Forssberg, H. (1999) Neural control of human motor development. *Curr Opin Neurobiol* **9**, 676–682.

Funakoshi, Y., Minami, M. & Tabata, T. (2001) *mtv* shapes the activity gradient of the Dpp morphogen through regulation of *thickveins*. *Dev* **128**, 67–74.

Gao, F.B., Brenman, J.E., Jan, L.Y. & Jan, Y.N. (1999) Genes controlling dendrite outgrowth, branching, and routing in *Drosophila*. *Genes Dev* **13**, 2549–2561.

Granato, M., van Eeden, F.J., Schach, U., Trowe, T., Brand, M., Furutani-Seiki, M., Haffter, P., Hammerschmidt, M., Heisenberg, C.P., Jiang, Y.J., Kane, D.A., Kelsh, R.N., Mullins, M.C., Odenthal, J. & Nusslein-Volhard, C. (1996) Genes controlling and mediating locomotion behavior of the zebrafish embryo and larva. *Development* **123**, 399–413.

Grillner, S. (1985) Neurobiological bases of rhythmic motor acts in vertebrates. *Science* **228**, 143–149.

Grillner, S., Cangiano, L., Hu, G.-Y., Thompson, R., Hill, R. & Wallen, P. (2000) The intrinsic function of a motor system – from ion channels to networks and behavior. *Brain Res* **886**, 224–236.

Gustafson, K. & Boulianne, G.L. (1996) Distinct expression patterns detected within individual tissues by the GAL4 enhancer trap technique. *Genome* **39**, 174–182.

Hoang, B. & Chiba, A. (2001) Single-cell analysis of Drosophila larval neuromuscular Synapses. *Dev Biol* **229**, 55–70.

Ito, K., Urban, J. & Technau, G.M. (1995) Distribution, classification, and development of *Drosophila* glial cells in the later embryonic and early larval ventral nerve cord. *Roux Arch Dev Biol* **204**, 284–307.

Jan, L.Y. & Jan, Y.N. (1976) Properties of the larval neuromuscular junction in *Drosophila melanogaster*. *J Physiol (Lond)* **262**, 189–214.

Kaminker, J.S., Canon, J., Salecker, I. & Banerjee, U. (2002) Control of photoreceptor axon target choice by transcriptional repression of Runt. *Nature Neuro* **5**, 746–750.

Keshishian, H., Broadie, K., Chiba, A. & Bate, M. (1996) The Drosophila neuromuscular junction: a model system for studying synaptic development and function. *Annu Rev Neurosci* **19**, 545–575.

Kitamoto, T. (2001) Conditional modification of behavior in *Drosophila* by targeted expression of a temperature-sensitive *shibire* allele in defined neurons. *J Neurobiol* **47**, 81–92.

LaJeunesse, D.R., McCartney, B.M. & Fehon, R.G. (2001) A systematic screen for dominant second-site modifiers of Merlin/NF2 phenotypes reveals an interaction with *blistered*/DSRF and *scribbler*. *Genet* **158**, 667–679.

Lee, T. & Luo, L. (1999) Mosaic analysis with a repressible cell marker for studies of gene function in neuronal morphogenesis. *Neuron* **22**, 451–461.

Li, H., Chaney, S., Forte, M. & Hirsh, J. (2000) Ectopic G-protein expression in dopamine and serotonin neurons blocks cocaine sensitization in *Drosophila melanogaster*. *Curr Biol* **10**, 211–214.

Lin, D.M. & Goodman, C.S. (1994) Ectopic and increased expression of Fasciclin II alters motorneuron growth cone guidance. *Neuron* **13**, 507–523.

Marder, E. (2000) Motor pattern generation. *Curr Opin Neurobiol* **10**, 691–698.

Marder, E. & Bucher, D. (2001) Central pattern generators and the control of rhythmic movements. *Curr Biol* **11**, R986–R996.

O'Brian, M.A. & Taghert, P.H. (1998) A peritracheal neuropeptide system in insects: release of myomodulin-like peptides at ecdysis. *J Exp Biol* **201**, 93–209.

Osterwalder, T., Yoon, K.S., White, B.H. & Keshishian, H. (2001) A conditional tissue-specific transgene expression system using inducible GAL4. *Proc Natl Acad Sci USA* **98**, 12596–12601.

Pearson, K.G. (1995) Proprioceptive regulation of locomotion. *Curr Opin Neurobiol* **5**, 786–791.

Rao, Y., Pang, P., Ruan, W., Gunning, D. & Zipursky, S.L. (2000) *brakeless* is required for photoreceptor growth-cone targeting in *Drosophila. Proc Natl Acad Sci USA* **97**, 5966–5971.

Ribera, A.B. & Nusslein-Volhard, C. (1998) Zebrafish touch-insensitive mutants reveal an essential role for the developmental regulation of sodium current. *J Neurosci* **18**, 9181–9191.

Rohrbough, J. & Broadie, K. (2002) Electrophysiological analysis of synaptic transmission in central neurons of *Drosophila* larvae. *J Neurophys* **88**, 847–860.

Salvaterra, P.M. & Kitamoto, T. (2001) *Drosophila* cholinergic neurons and processes visualized with Gal4/UAS-GFP. *Gene Expr Patterns* **1**, 73–82.

Sanes, D.H., Reh, T.A. & Harris, W.A. (2000) Behavioral development. In Sanes, D.H., Reh, T.A. & Harris, W.A. (eds), *Development of the Nervous System. Academic Press, San Diego, CA, pp. 404–452.*

Schneider, L.E., Sun, E.T., Garland, D.J. & Taghert, P.H. (1993) An immunocytochemical study of the FMRFamide neuropeptide gene products in *Drosophila. J Comp Neurol* **337**, 336–460.

Senti, K.-A., Keleman, K., Eisenhaber, F. & Dickson, B.J. (2000) *brakeless* is required for lamina targeting of R1–R6 axons in the *Drosophila* visual system. *Development* **127**, 2291–2301.

Sepp, K.J. & Auld, V.J. (1999) Conversion of *lacZ* enhancer trap lines to *Gal4* lines using targeted transposition in *Drosophila melanogaster. Genetics* **151**, 1093–1101.

Shaver, S.A., Riedl, C.A., Parkes, T.L., Sokolowski, M.B. & Hilliker, A.J. (2000) Isolation of larval behavioral mutants in *Drosophila melanogaster. J Neurogenet* **14**, 193–205.

Shiga, Y., Tanaka-Matakatsu, M. & Hayashi, S. (1996) A nuclear GFP/beta- galactosidase fusion protein as a marker for morphogenesis in living *Drosophila. Dev Growth Diffn* **38**, 99–106.

Siegmund, T. & Korge, G. (2001) Innervation of the ring gland of *Drosophila melanogaster. J Comp Neurol* **431**, 481–491.

Sillar, K.T. & Roberts, A. (1993) Control of frequency during swimming in Xenopus embryos: a study on interneuronal recruitment in a spinal rhythm generator. *J Physiol* **472**, 557–572.

Stewart, B.A., Atwood, H.L., Renger, J.J., Wang, J. & Wu, C.-F. (1994) Improved stability of *Drosophila* larval neuromuscular preparations in haemolymph-like physiological solutions. *J Comp Physiol* **A 175**, 179–191.

Sun, B., Xu, P., Wang, W. & Salvaterra, P.M. (2001) In vivo modification of Na^+, K^+ -Atpase activity *Drosophila. Comp Biochem Physiol, Part B* **130**, 521–536.

Suster, M.L. & Bate, M. (2002) Embryonic assembly of a central pattern generator without sensory input. *Nature* **416**, 174–178.

Suster, M.L., Martin, J.R., Sung, C. & Robinow, S. (2003) Targeted expression of tetanus toxin reveals sets of neurons involved in larval locomotion in *Drosophila. J Neurobiol* **55**, 233–246.

Sweeney, S.T., Broadie, K., Keane, J., Niemann, H. & O'Kane, C.J. (1995) Targeted expression of tetanus toxin light chain in *Drosophila* specifically eliminates synaptic transmission and causes behavioral deficits. *Neuron* **14**, 341–351.

Taghert, P.H., Hewes, R.S., Park, J.H., O'Brien, M.A., Han, M. & Peck, M.E. (2001) Multiple amidated neuropeptides are required for normal circadian locomotor rhythms in *Drosophila. J Neurosci* **21**, 6673–6686.

Thor, S., Andersson, S.G., Tomlinson, A. & Thomas, J.B. (1999) A LIM-homeodomain combinatorial code for motor-neuron pathway selection. *Nature* **397**, 76–80.

Wang, J.W., Sylwester, A.W., Reed, D., Wu, D.A., Soll, D.R. & Wu, C.F. (1997) Morphometric description of the wandering behavior in *Drosophila* larvae: aberrant locomotion in Na and K channel mutants revealed by computer- assisted motion analysis. *J Neurogenet* **11**, 231–254.

White, B.H., Osterwalder, T.P., Yoon, K.S., Joiner, W.J., Whim, M.D., Kaczmarek, L.K. & Keshishian, H. (2001) Targeted attenuation of electrical activity in *Drosophila* using a genetically modified K (+) channel. *Neuron* **31**, 699–711.

Wolf, E. & Roberts, A. (1995) The influence of premotor interneuron populations on the frequency of the spinal pattern generator for swimming in Xenopus embryos: a simulation study. *Eur J Neurosci* **7**, 671–678.

Yang, P., Shaver, S.A., Hilliker, A.J. & Sokolowski, M.B. (2000) Abnormal turning behavior in *Drosophila* larvae. Identification and molecular analysis of *scribbler* (*sbb*). *Genetics* **155**, 1161–1174.

Zito, K., Fetter, R.D., Goodman, C.S. & Isacoff, E. (1997) Synaptic clustering of Fasciclin II and Shaker: essential targeting sequences and role of *dlg. Neuron* **19**, 1007–1016.

Acknowledgments

Work was funded by grants from the Natural Science and Engineering Research Council of Canada to M.B.S and H.L.A and by the Canada Research Chair Program and the Canadian Foundation for Innovation to M.B.S. M.L.S thanks the Venezuelan National Academy of Sciences for financial support. We are grateful to Michael Bate in whose laboratory this work was initiated and Irmtraut Rathjens for excellent technical assistance and Gregory Macleod for helpful comments on the manuscript. We thank Brian McCabe, Paul Taghert, Thomas Siegmund, Thomas Osterwalder, Kei Ito and many others who provided valuable *Drosophila* stocks. We also thank the following colleagues for generously providing us primary antibodies: Barry Dickson (mouse anti-BKS), Yong Rao (rabbit anti-BKS), John Carlson and Wayne Johnson (anti-ACJ6), Paul Salvaterra (anti-ChAT), Paul Taghert (anti-FMRFamide and anti-PHM), and Michael Bate (anti-EVE, anti-FASII and anti-REPO). Mouse 22C10 and anti-ELAV (9F8A9) antibodies were obtained from the Developmental Studies Hybridoma Bank, Iowa City, IA.